ENVIRONMENTAL RESEARCH
LETTERS

LETTER • OPEN ACCESS

Increasing confidence in projecting the Arctic ice-free year with emergent constraints

To cite this article: Bin Wang *et al* 2021 *Environ. Res. Lett.* **16** 094016

View the article online for updates and enhancements.

This content was downloaded from IP address 141.239.154.39 on 03/10/2021 at 07:26

ENVIRONMENTAL RESEARCH
LETTERS

OPEN ACCESS

RECEIVED
29 January 2021

REVISED
6 June 2021

ACCEPTED FOR PUBLICATION
14 June 2021

PUBLISHED
18 August 2021

Original content from this work may be used under the terms of the Creative Commons Attribution 4.0 licence.

Any further distribution of this work must maintain attribution to the author(s) and the title of the work, journal citation and DOI.

LETTER

Increasing confidence in projecting the Arctic ice-free year with emergent constraints

Bin Wang[1,2,*], **Xiao Zhou**[1], **Qinghua Ding**[3] **and Jiping Liu**[4]

[1] Department of Atmospheric Sciences, the University of Hawaii at Manoa, Honolulu, HI 96822, United States of America
[2] Erath System Modeling Center, Nanjing University of Information Science and Technology, Nanjing 210024, People's Republic of China
[3] Department of Geography, Earth Research Institute, University of California, Santa Barbara, Santa Barbara, CA 93106, United States of America
[4] Department of Atmospheric and Environmental Sciences, State University of New York, Albany, NY 12222, United States of America
[*] Author to whom any correspondence should be addressed.

E-mail: wangbin@hawaii.edu

Keywords: sea ice area, sea ice extent, climate sensitivity, emergent constraint, first Arctic ice-free year, CMIP6 model, projection uncertainty

Supplementary material for this article is available online

Abstract

An ice-free Arctic summer is a landmark of global change and has the far-reaching climate, environmental, and economic impacts. However, the Coupled Model Intercomparison Project Phase 6 models' projected occurrence remains notoriously uncertain. Finding emergent constraints to reduce the projection uncertainties has been a foremost challenge. To establish a physical basis for the constraints, we first demonstrate, with numerical experiments, that the observed trend of Arctic ice loss is primarily driven by the Arctic near-surface air temperature. Thus, two constraints are proposed: the Arctic sea ice sensitivity that measures Arctic sea ice response to the local warming, and the Arctic amplification sensitivity that assesses how well the model responds to anthropogenic forcing and allocates heat to the Arctic region. The two constraints are complementary and nearly scenario-independent. The model-projected first Arctic ice-free year significantly depends on the model's two climate sensitivities. Thus, the first Arctic ice-free year can be predicted by the linear combination of the two Arctic sensitivity measures. Based on model-simulated sensitivity skills, 20 CMIP models are divided into two equal number groups. The ten realistic-sensitivity models project, with a likelihood of 80%, the ice-free Arctic will occur by additional 0.8 °C global warming from 2019 level or before 2040 under the SSP2-4.5 (medium emission) scenario. The ten realistic-sensitivity models' spread is reduced by about 70% compared to the ten underestimate-sensitivity models' large spread. The strategy for creating physics-based emergent constraints through numerical experiments may be instrumental for broad application to other fields for advancing robust projection and understanding uncertainty sources.

1. Introduction

An ice-free Arctic summer is the most iconic symbol of global warming. Arctic sea ice extent (SIE), defined as the area where the ice concentration is higher than 15% in a given area, shows a drastic decline in September since the late 1970s (Comiso *et al* 2008, Cavalieri and Parkinson 2012), reaching a historical record low on 16 September 2012 (3.41 million km^2) (Liu *et al* 2013) and the second-lowest minimum in 2020 (Gautier 2020). How soon the summer Arctic will become ice-free is a keen societal concern as the ice-free Arctic may have remarkable impacts on the Arctic environment, marine ecosystem, and maritime activities. Meanwhile, it may create enormous economic risks and opportunities (Smith and Stephenson 2013, He and Hu 2018). The ice-free Arctic may also affect the extreme weather and climate in lower latitudes (Overland *et al* 2011, Francis and Vavrus 2012, Cohen *et al* 2019).

© 2021 The Author(s). Published by IOP Publishing Ltd

The climate/earth system models' projected occurrence of the first Arctic ice-free summer, however, has remained notoriously uncertain in the past two decades. The most recent Coupled Model Intercomparison Project Phase 6 (CMIP6) models projected the ice-free Arctic could occur as early as 2015 and as late as far beyond 2100 (Notz *et al* 2020). Therefore, constraining and selecting models to reduce the uncertainty arising from model physics and emission scenarios have been a foremost challenge in predicting the future change of sea ice.

The model selection has been based on the quality of the simulated sea ice climatology (mean and seasonal cycle) and the trend of Arctic September SIE (Wang and Overland 2009, 2012, Stroeve *et al* 2012, Liu *et al* 2013, Snape and Forster 2014). These selections involved extrapolation (Wang and Overland 2009, 2012) and calibration (Snape and Forster 2014) based on observed trends. Thus, the projections vary with the calibration periods because observed trends are affected by internal variability (Kay *et al* 2011).

An effective way to reduce the uncertainties is to develop emergent constraints by finding links between the inter-model spread in an observable predictor and climate projections (Brient 2020). Examples are the Arctic September sea ice area (SIA) sensitivity to a given amount of global warming (Mahlstein and Knutti 2012, Stroeve and Notz 2015, Gregory *et al* 2002) and/or to a given amount of accumulative anthropogenic CO_2 emission (Herrington and Zickfeld 2014, Notz and Stroeve 2016, Notz 2020). These sensitivity constraints measure models' fidelity in reproducing the local Arctic SIA's response to global external forcing. Nevertheless, any local response is driven by atmospheric circulation and varies from place to place, even under the same external global forcing. Besides, the Arctic sensitivities to the worldwide emission of CO_2 and global warming are highly related; most models cannot capture these sensitivities realistically, making selecting models intricate (Notz 2020). Recently, Massonnet *et al* (2018) showed that the seasonal sea ice melting and growth efficiency, and hence SIA and volume, strongly depend on the background thickness. Ideally, an observational constraint on the simulated volume projections might be desirable. Unfortunately, as they pointed out, the lack of long-term and reliable sea-ice volume observations makes it impossible to reduce the spread in the projected Arctic sea-ice volume loss significantly. Thackeray and Hall (2019) used models-simulated seasonal variations of sea ice-albedo feedback (SIAF) as an emergent constraint. Although the seasonal SIAF is correlated with future change SIAF, this relationship can only apply to the near future projection and is sensitive to the historical sea ice thickness.

The primary science question to be addressed here is how to develop physics-based emergent constraints independent of scenarios and complementary to each other so that the projected uncertainties could be effectively reduced. We consider it crucial to justify the physical basis for the proposed constraints. For this purpose, we first conducted a suite of numerical experiments to demonstrate that the Arctic near-surface air temperature is the primary driver for the observed trend of Arctic ice loss. As such, a reliable model should reproduce a realistic Arctic sea ice response to the local warming and redistribute an adequate amount of heat to the Arctic region in response to anthropogenic forcing-induced global warming. The physical reasoning here leads to two complementary emergent constraints. We then show they are scenario-independent and could significantly reduce the projected uncertainties due to model physics. In contrast to previous efforts, this new approach emphasizes the physical consideration for seeking independent constraints that place Arctic sea ice loss in the context of global-scale temperature variability.

2. Data and method

The word 'ice-free' has been quantitatively defined by the Arctic SIE being less than 1.0 million km^2 (Wang and Overland 2009, 2012, Liu *et al* 2013). The 'ice-free' is recently defined by the Arctic SIA being less than 1.0 million km^2 (Snape *et al* 2014, Notz 2020). The SIA is the sum of the pixel area multiplied by sea ice concentration across all sea ice grids with a fraction greater than 15%. The SIA better reflects the Arctic ice albedo and ice concentration (Snape and Forster 2014). In this study, we adopt the SIA criterion for 'ice-free'. However, we also conduct parallel computation using the SIE criterion to compare with published works that used SIE as a criterion. We find a significant relationship between the SIE and SIA in observation and in models, namely, the Arctic September SIA is about 1 million km^2 smaller than the corresponding SIE (see supplementary material (available online at stacks.iop.org/ERL/16/094016/mmedia)). Thus, the first Arctic ice-free year depends on the definition of 'ice-free'.

2.1. Data

We used the National Snow and Ice Data Centre sea ice index, which is derived by using measurements from the Special Sensor Microwave/Imager sensors on the Defence Meteorological Satellite Program-F8, -F11, and -F13 satellites. The dataset is generated using the Advanced Microwave Scanning Radiometer-Earth Observing System Bootstrap Algorithm with daily varying tie-points from November 1978 through December 2018. The Northern Hemisphere sea ice concentration data (version 3.1, update in 2018) is mapped to a standard rectangular

grid overlaid on a north polar stereographic projection with a grid size of 25 × 25 km (Comiso 2017). Due to the satellite orbit inclination, there is a central Arctic hole in the raw data. To keep the data's consistency, we patched the holes using the average value of the northernmost latitude. Then, the monthly SIA is calculated based on sea ice concentration.

The 2 m near-surface air temperature is also used to diagnose the Arctic temperature amplification ratio and the sea ice sensitivity to Arctic warming. To reduce the uncertainty in the monthly mean 2 m air temperature over the Arctic, we used the ensemble mean of two reanalysis datasets: the fifth generation European Centre for Medium-Range Weather Forecasts (ECMWF) reanalysis data (ERA-5) with 1° resolution from the ECMWF (Hersbach *et al* 2019) and the National Centres for Environmental Prediction (NCEP-II) datasets with 2.5° resolution (Kanamitsu *et al* 2002). The period of 1979–2014 is chosen as the evaluation period as it overlaps with the satellite observation period, and 2014 is the last year of the models' historical simulation period.

2.2. CMIP6 models

We analyze 20 CMIP6 models on the Earth System Grid Federation. It is desirable to include more models to estimate the range of uncertainty. However, to examine the scenario dependence of the proposed constraints, we used only 20 models that contain four-scenario projections. The SSP2-4.5 and SSP5-8.5 scenario represents a medium and high radiative forcing of 4.5 and 8.5 W m^{-2} in 2100 relative to the pre-industrial levels. These two scenarios can be comparable with RCP-4.5 and RCP-8.5 for CMIP5, respectively. Another two scenarios of SSP1-2.6 and SSP3-7.0 are also used to test the sea ice sensitivity. Among these 20 models, most models provide more than one realization. Therefore, we used as many realizations as possible to reduce the effect of internal variability.

2.3. The sea ice model

The sea ice model used to perform the experiments in this study is the Los Alamos sea ice model (CICE5) (Hunke *et al* 2017) with a horizontal resolution of (320 × 384) and seven vertical levels of sea ice (supplementary information). Since an identical initial state of sea ice is crucial for this study, we firstly perform a 200 year run with the fixed 1979 year atmospheric and oceanic transient forcing to spin up the ocean and get a steady-state. We take the mean value of the last 50 years as an initial condition for all control and sensitivity experiments. Then, a 40 year control (CTRL) simulation is performed with the observed time-varying atmospheric (every 6 h) and oceanic (every month) forcing from 1979 to 2018.

3. Result

3.1. Physical consideration for the new Arctic climate sensitivity constraints

We argue that T2m in May–June–July–August (MJJA) can control the variability of September Sea ice by shaping downward longwave radiation (DLR) in summer. The DLR is a key term to determine Net radiation, Qnet, and sea ice changes in the melting season. Figure 1(a) shows that the T2m, DLR, and Qnet co-very well with the September SIA over the period, with the trends either removed or retained. DLR is also highly sensitive to T2m ($r = 0.88$), as we expect based on the empirical formula used in CICE5 (Idso and Jackson, 1969). In particular, DLR has the strongest correlation with Qnet and the largest mean value (about 286 W m^{-2}) and standard deviation in summer, compared with the other five fluxes at the surface, suggesting its key role in bridging atmospheric forcing (reflected by T2m here) to sea ice. The DLR is primarily determined by the t2m, though the cloud plays a minor role. As far as we know, this result is not explicitly discussed in previous studies (e.g. Ding *et al* 2017, Olonscheck *et al* 2019).

To support the hypothesis mentioned above, we conducted a suite of numerical experiments with the CICE5 model (see supplementary information). The model's control run with the observed time-varying atmospheric and oceanic forcing from 1979 to 2018 can capture the declining trend, and year-to-year variations of the observed September Arctic SIA except for an overestimate in the beginning years (figure 1(b)). In the T2m-only experiment, the time-varying 2 m air temperature is applied, while the linear trends of all other forcing variables are removed. The model can generally reproduce the declining trend and variability of the September Arctic SIA, suggesting the essential role of the 2 m air temperature (figure 1(b)). In the T2m-detrend experiment, the linear trend for 2 m air temperature is removed, but all other atmospheric forcing variables are kept the same as in the control run. The SIA declining trend, in this case, is substantially reduced, suggesting that the other time-varying atmospheric forcings together play a minor role in generating the declining trend. Seven additional sensitivity experiments are performed to identify the impacts of each atmospheric forcing. The results from seven additional experiments that identify the role of each atmospheric forcing variable confirm that the 2 m air temperature and temperature-related moisture variability contribute the most to the September SIA's declining trend, while other atmospheric forcing-induced trends are an order of magnitude smaller (supplementary figure 1). Further experiment result suggests that the role of ocean forcing is insignificant in the simulation of the SIA trends (supplementary information). The experimental results reveal that the

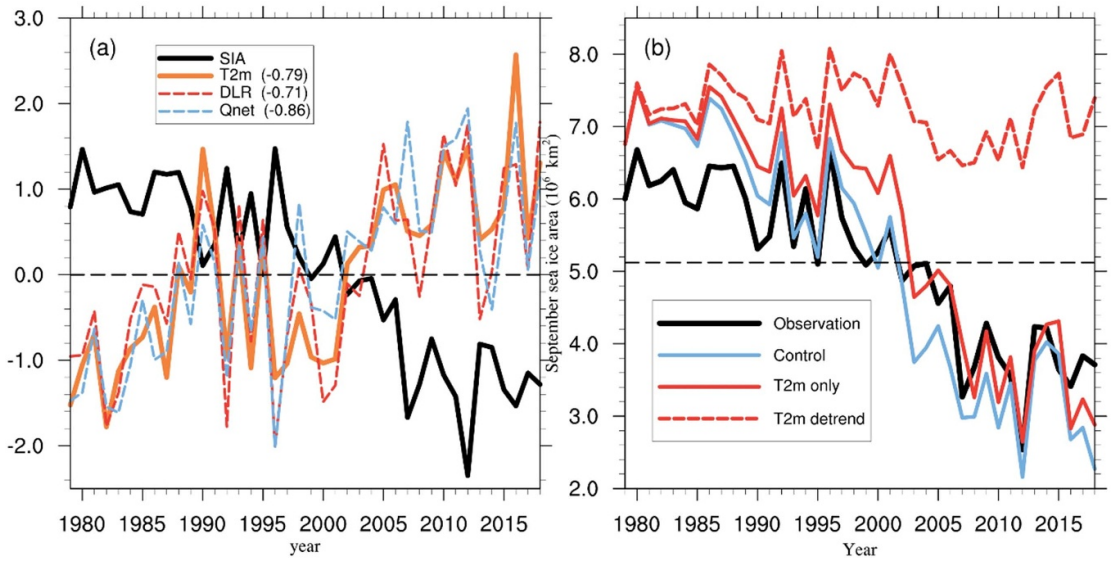

Figure 1. (a) Time series (standardized) of domain average of September SIA, MJJA T2m, DLR, and net radiation (Qnet) over the Arctic Ocean derived from observation. The value in the bracket shows the correlation of each heat flux with SIA. (b) Numerical experiment results showing the dominant role of the Arctic surface air temperature in driving SIA variability. September SIA obtained from observation (solid black curve), control run (solid blue curve), 2 m air temperature only experiment (solid red curve), and 2 m air temperature detrend experiment (dashed red curve). The dashed black line shows the observed September mean SIA during 1979–2018.

Arctic atmospheric surface temperature change plays a dominant role in generating the recent trend and variability of the September Arctic SIA.

3.2. Two complementary Arctic climate sensitivity constraints

Considering that Arctic near-surface air temperature is a primary driver for the observed Arctic SIA variability, a reliable model should reproduce correctly Arctic SIA sensitivity defined by the simulated declining rate of the September Arctic SIA to given one degree Celsius of summer Arctic mean surface temperature (AMST). The summer here means MJJA because the maximum sea ice melting rate occurs in June and July (supplementary figure 2). The model physics-dependent Arctic SIA sensitivity is estimated by the least-square regression between the MJJA Arctic mean 2 m air temperature and September Arctic SIA using historical experiment data for 1979–2014 (supplementary figure 3). The correlations between them are generally significant at the 95% confidence level in most CMIP6 models, which corroborates the linear relationship between SIA decline and temperature increase found by Mahlstein and Knutti (2012).

Arctic warming is linked to global warming. The warming outside of the Arctic can influence the Arctic region through atmospheric teleconnections (Grunseich and Wang 2016a, 2016b) and northward heat transports via atmospheric and oceanic processes and through triggering local processes and feedbacks (sea ice-albedo-temperature feedback, changes in cloud cover, water vapor, temperature's lapse rate, and heat-absorbing aerosols in snow) further amplifying the Arctic warming (the Arctic amplification) (Curry *et al* 1995, Serreze and Francis 2006, Graversen *et al* 2008, Shindell and Faluvegi 2009, Döscher *et al* 2014). Thus, a reliable projection model is expected to reproduce a realistic summer AMST response to a given amount of global warming (Arctic amplification ratio). Therefore, we define Arctic temperature sensitivity by the simulated summer AMST to given one degree Celsius of summer global mean surface temperature (GMST). Arctic temperature sensitivity is estimated by the regressions between the simulated MJJA AMST and observed MJJA GMST from 1979 to 2014 (supplementary figure 3). Note that the trends of summer GMST are nearly the same as that of annual mean GMST. Here we take global warming as a proxy of the anthropogenic radiative forcing as the GMST is a crucial indicator of global change, and it better reflects the global impacts of the anthropogenic forcing (Notz 2020).

The September Arctic SIA sensitivity assesses how the sea ice model captures the sea ice melting to the local atmospheric forcing, evaluating how well a sea ice model is. The Arctic summer temperature sensitivity assesses how good the model responds to anthropogenic forcing and how well the model's dynamic processes allocate heat to the Arctic region. Together, they assess the models' fidelity in the simulated response of the September Arctic SIA to the observed global warming.

For any proposed constraints, scenario independence is a desirable property as it could minimize the uncertainty arising from the assumed scenarios. Although previous studies have shown the projected first ice-free Arctic is scenario-independent (e.g. Jahn 2018, Sigmond *et al* 2018, Notz 2020). It is

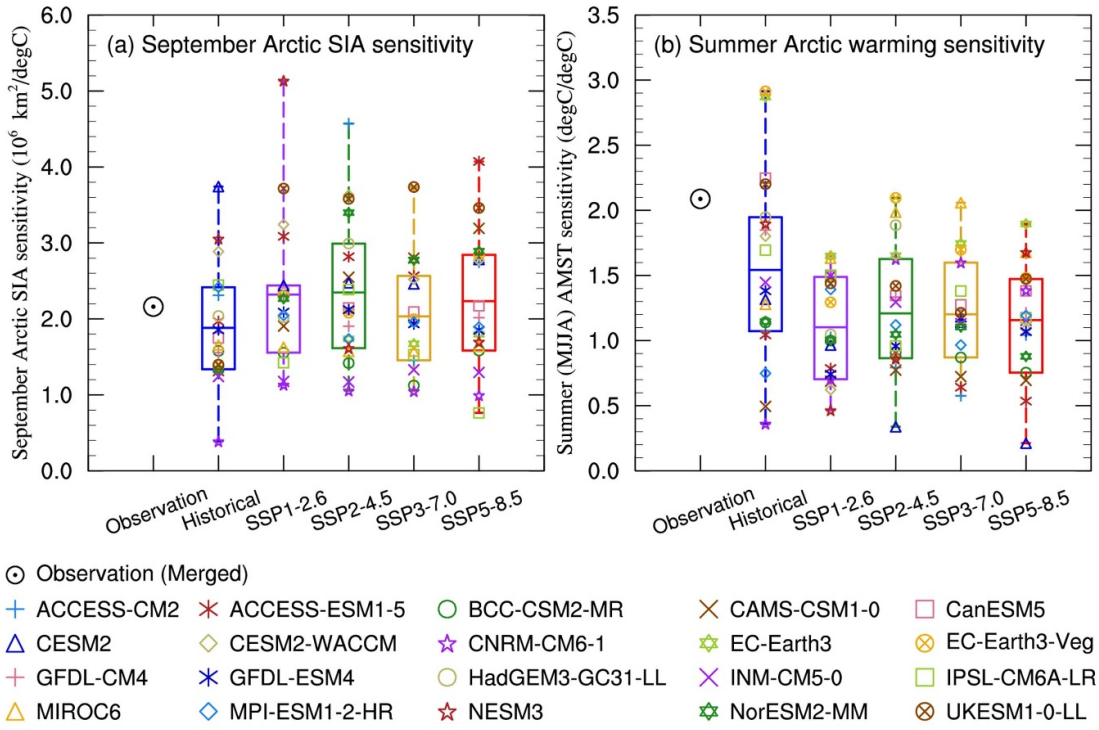

Figure 2. Scenario-independent Arctic climate sensitivity constraints. (a) September SIA sensitivity to summer (MJJA) AMST, for observation, historical experiment, SSP1-2.6, SSP2-4.5, SSP3-7.0, and SSP5-8.5 scenarios, respectively. The box plot shows the uncertainty measured by the inter-model spread. The upper (lower) edge of the box represents the 83rd (17th) percentile, so the box contains 66% of the model projection data and represents the 'likely' range. The horizontal line within the box is the mean value. The vertical dash line segments represent the 'very likely' range from 5% to 95%. (b) The same as in (a) except for the sensitivity of summer (MJJA) AMST to the summer GMST. For historical simulation, observed GMST is used. For projection, the model projected GMST is used.

unknown whether the proposed sensitivity measures vary with emission scenarios. Figure 2(a) compares the SIA sensitivities derived from observations and each model in their historical simulations and future projections. From 1979 to 2014, the observed Arctic SIA sensitivity is 2.16 million km^2 °C^{-1}. The models-simulated mean Arctic SIA sensitivity (1.88 million km^2 °C^{-1}) is 12.9% lower. Under the four different CMIP6 scenarios, the Arctic SIA sensitivities projected by the 20-models' ensemble averages are almost the same (~2.23 million km^2 °C^{-1}) (figure 2(a)), indicating that the projected SIA climate sensitivity is nearly scenario-independent. This assertion is supported by the high correlation in the SIA sensitivity between the SSP2-4.5 and SSP5-8.5 runs (supplementary figure 4(a)), confirming that the SIA sensitivity does not appreciably vary with the emission scenarios. The projected sensitivity tends to be higher than those in historical simulations because the volcano forcing used in the historical run might reduce Arctic warming (Rosenblum and Eisenman 2016) and because ice-albedo feedback, higher Arctic temperatures, and thinning ice pack in the future could accelerate the decline rate (Stroeve *et al* 2011).

Similar to the Arctic SIA sensitivity, the models-simulated mean Arctic temperature sensitivity (1.54) is about 26.1% lower than the observed (figure 2(b)). In future projections, the 20-model averaged Arctic temperature sensitivity under the four different CMIP6 scenarios is also nearly invariant (~1.17). The future projected amplification ratio is close to the models' simulated amplification ratio during 1979–2014 (1.29). However, it is significantly lower than the Arctic temperature sensitivity during 1979–2014 (1.54) because the 1979–2014 Arctic temperature sensitivity is calculated based on the observed global mean t2m, whereas in the future scenario, it is calculated using the model projected global mean t2m, which represents the Arctic amplification ratio that is determined by the models' internal variability only. The higher sensitivity during 1979–2014 is due to the observed global mean temperature is lower than the model-simulated counterpart.

In addition to scenario-independent, the two sensitivity constraints are independent of each other, as evidence by their correlation coefficient of 0.06, adding strength to their combined use.

3.3. Future projection of the first Arctic ice-free year

The inter-model spread in 20 CMIP6 models-projected first ice-free Arctic year ranges from 2019 to far beyond 2100 with a mean of 2068 under the medium emission (SSP2-4.5) scenario (figure 3). We use the Arctic SIA sensitivity and Arctic temperature sensitivity as two criteria to select credible models

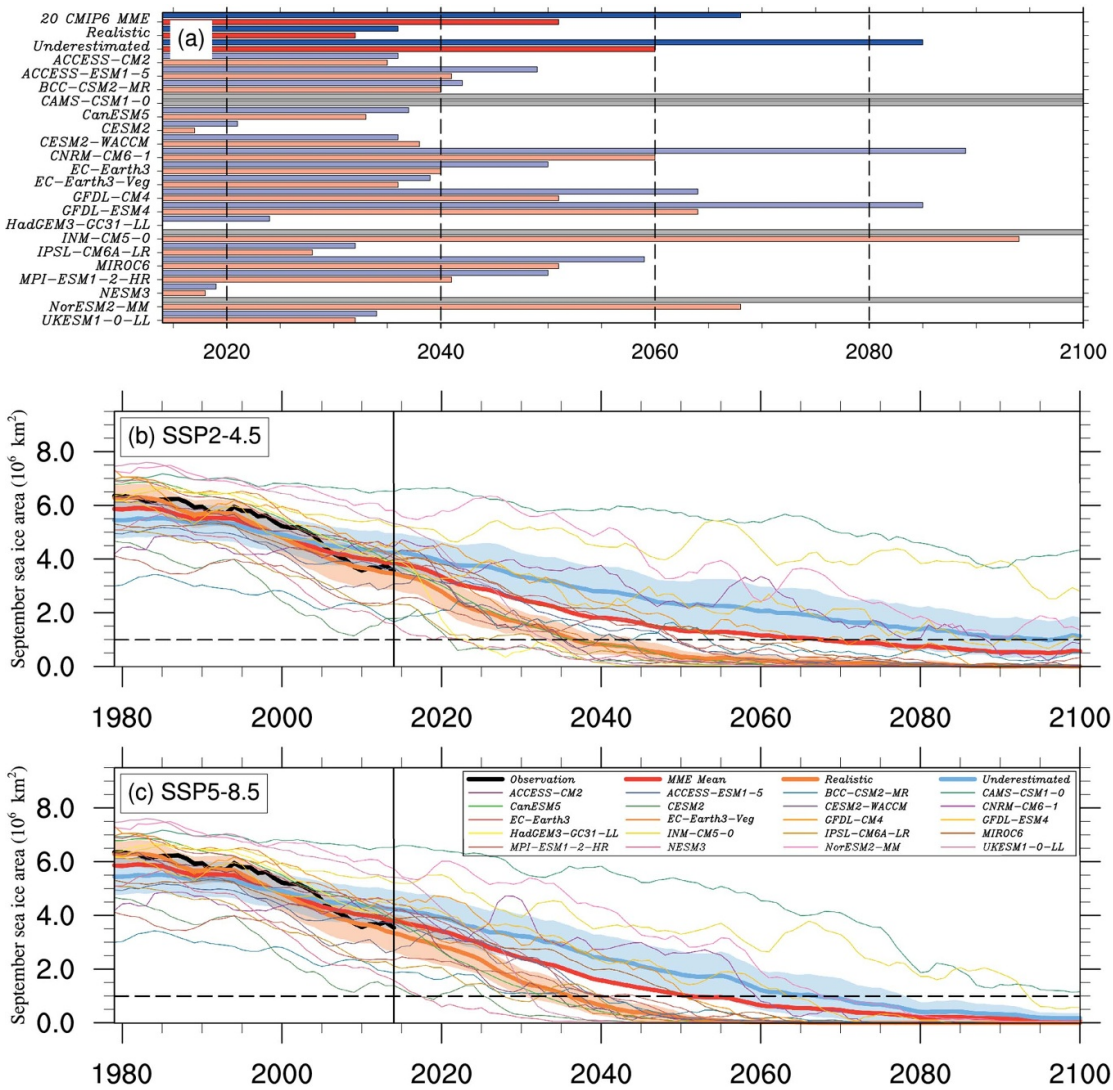

Figure 3. CMIP6 models' projections of the first Arctic ice-free years. (a) The first ice-free year projected by 20 individual CMIP6 models, the 20-model ensemble mean, and the ensemble means of the ten realistic-sensitivity models and ten underestimated-sensitivity models, respectively, under the SSP2-4.5 (blue or light blue colour) and the SSP5-8.5 (red or brown colour) scenarios. (b) and (c) Time-series of the simulated (1979–2014) and projected (2015–2100) September SIA by 20 individual CMIP6 models under the (b) SSP2-4.5 scenario and (c) SSP5-8.5 scenario. The thick black curve is the observation; the thick red curve is the 20 models' multi-model ensemble mean. The thick brown and blue curves are MME of ten realistic-sensitivity models and ten underestimated-sensitivity models, respectively. The shading region shows the uncertainty of each group (defined as one standard deviation of inter-model spread). Five-year running mean has been applied to the data.

to reduce the uncertainty. We first selected models having the best match to the observed sensitivities, resulting in seven models (figure 4(a)). To facilitate comparison, we have used the projected last 30 year trend to extrapolate its occurrence for the cases where the projected year is beyond 2100. The seven models' ensemble projects the averaged first ice-free year in 2036 under the SSP2-4.5 scenario with one standard deviation of the model spread of 14 years that is one-third of the 20 models' spread (43 years).

One may argue that the reduced uncertainty is due to the uneven numbers of models under comparison. For a fairer comparison, we divide 20 models into two equal number groups. This division is made by the dashed red line in figure 4(a), which crosses the models' ensemble mean sensitivity and perpendicular to the segment connecting the models' ensemble mean (red dot) and observation (black dot). The division yields an above-average (right of the red line) and a below-average (left of the red line) group with ten models in each. Since the observation is located to the right of the red line, the ten above-average models are referred to as 'realistic-sensitivity' models, while the ten below-average models are called 'underestimated-sensitivity' models. The ten realistic models are marked by red color in the legend.

Figure 4(b) shows that the ten realistic-sensitivity models project a mean first ice-free year in 2036 (2032) with one standard deviation of the inter-model spread of 14 (10) years and the range of spread of 2019–2064 (2018–2051) under the SSP2-4.5 (SSP5-8.5) scenario. This result is nearly the same as

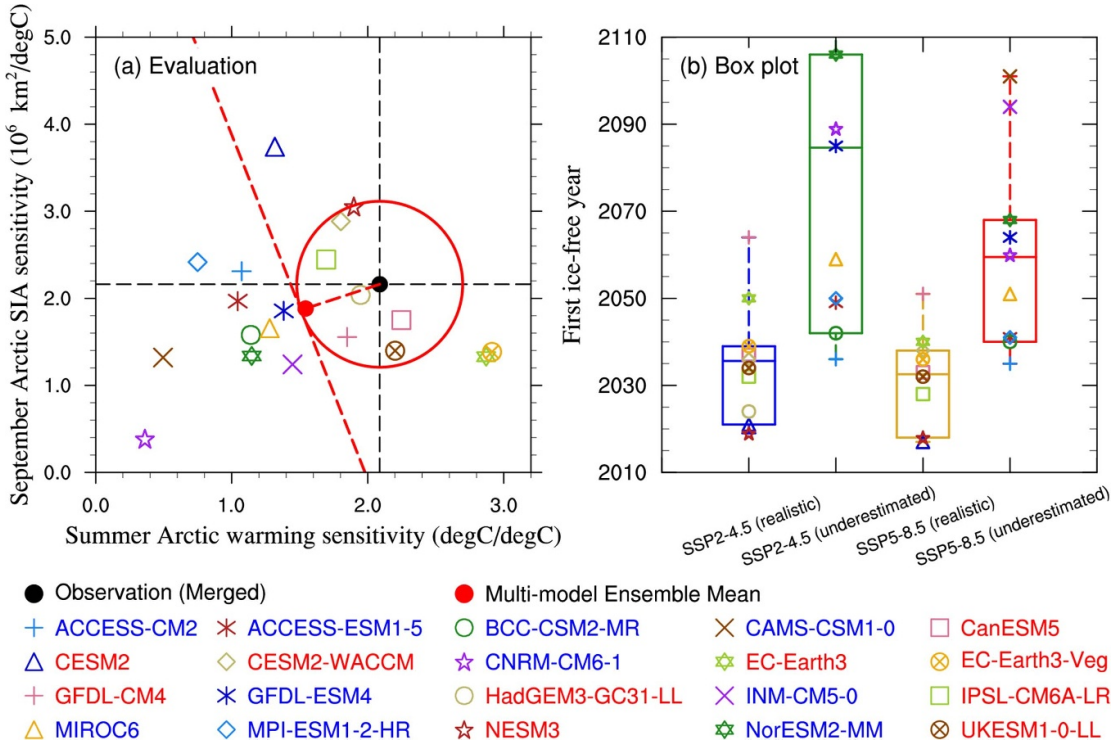

Figure 4. Comparison of the projections made by realistic-sensitivity and underestimated-sensitivity models. (a) Evaluation of SIA performance in each CMIP6 model by two metrics. The abscissa is the Arctic warming sensitivity defined by the simulated summer (MJJA) AMST to one-degree Celsius observed summer GMST. The ordinate is September Arctic SIA sensitivity to one-degree Celsius Arctic warming. The black and red dots denote observed and 20 models' MME, respectively. The seven models within the red circle are the best performing models. The ten models to the right of the red dashed line denote realistic-sensitivity models (names marked by red in the legend), while the ten models to the left of the dashed line are underestimated-sensitivity models (marked by blue in the legend). (b) The first Arctic ice-free year projected under SSP2-4.5 (left) and SSP5-8.5 (right) scenarios. The two box plots compare the ten realistic-sensitivity models and ten underestimated-sensitivity models' projection for each scenario.

the seven best model's ensemble projections. In contrast, the ten underestimated-sensitivity models project an averaged first ice-free year in 2085 (2060) with one standard deviation of the spread of 48 (23) years and the full range of spread of 2036–2172 (2035–2101) under the SSP2-4.5 (SSP5-8.5) scenario. Thus, the standard deviation of the ten realistic models' spread reduces to about 30% of the ten underestimate models' counterparts under the SSP2-4.5 scenario.

Different constraints used in the previous studies are compared with ours in terms of the intermodel spread. These constraints include (a) the simulated mean September SIA/extent (Wang and Overland 2009, 2012, Stroeve *et al* 2012, Massonnet *et al* 2018; Liu *et al* 2013), (b) the linear trend of September SIA (Liu *et al* 2013, Massonnet *et al* 2018), (c) the September Sea ice sensitivity to a given one-degree global mean surface air temperature increase (Notz *et al* 2020). We selected the top ten models from the same 20 CMIP6 models based on each constraint for a fair comparison. The results show that the standard deviations (ranges) of the intermodal spread under the SSP2-4.5 scenario are 38 years (2024–2158), 20 years (2021–2085), and 19 years (2019–2085) for the above-mentioned constraints (a), (b), and (c), respectively. Thus, for the same number of selected best models, the ice-free year of MME based on the constraints proposed in this study shows the smallest intermodal spread and uncertainty range.

The inter-model spread analysis unravels that the model-projected first Arctic ice-free year critically depends on the model's two climate sensitivity measures (figure 5). Under the SSP5-8.5 scenario, the models-projected first Arctic ice-free years are significantly correlated with the observed September Arctic SIA sensitivity ($r = -0.62$, $p < 0.05$) and the summer Arctic temperature sensitivity ($r = -0.44$, $p < 0.05$), respectively (figure 5). Therefore, the models' projected ice-free years can be estimated by the complex regression of the two models' Arctic sensitivities with a correlation skill of 0.73 ($p < 0.01$):

$$\begin{aligned}&\text{First ice-free year}\\&\quad = 2047—16.9(\text{SIAsensitivity}—1.9)\\&\qquad\quad —12.8(\text{Arctic warming sensitivity}—1.5).\end{aligned}$$

This approximate equation, with ten realistic models' mean sensitivity, yields the first ice-free year of 2035, roughly consistent with the ten realistic model's ensemble mean projection.

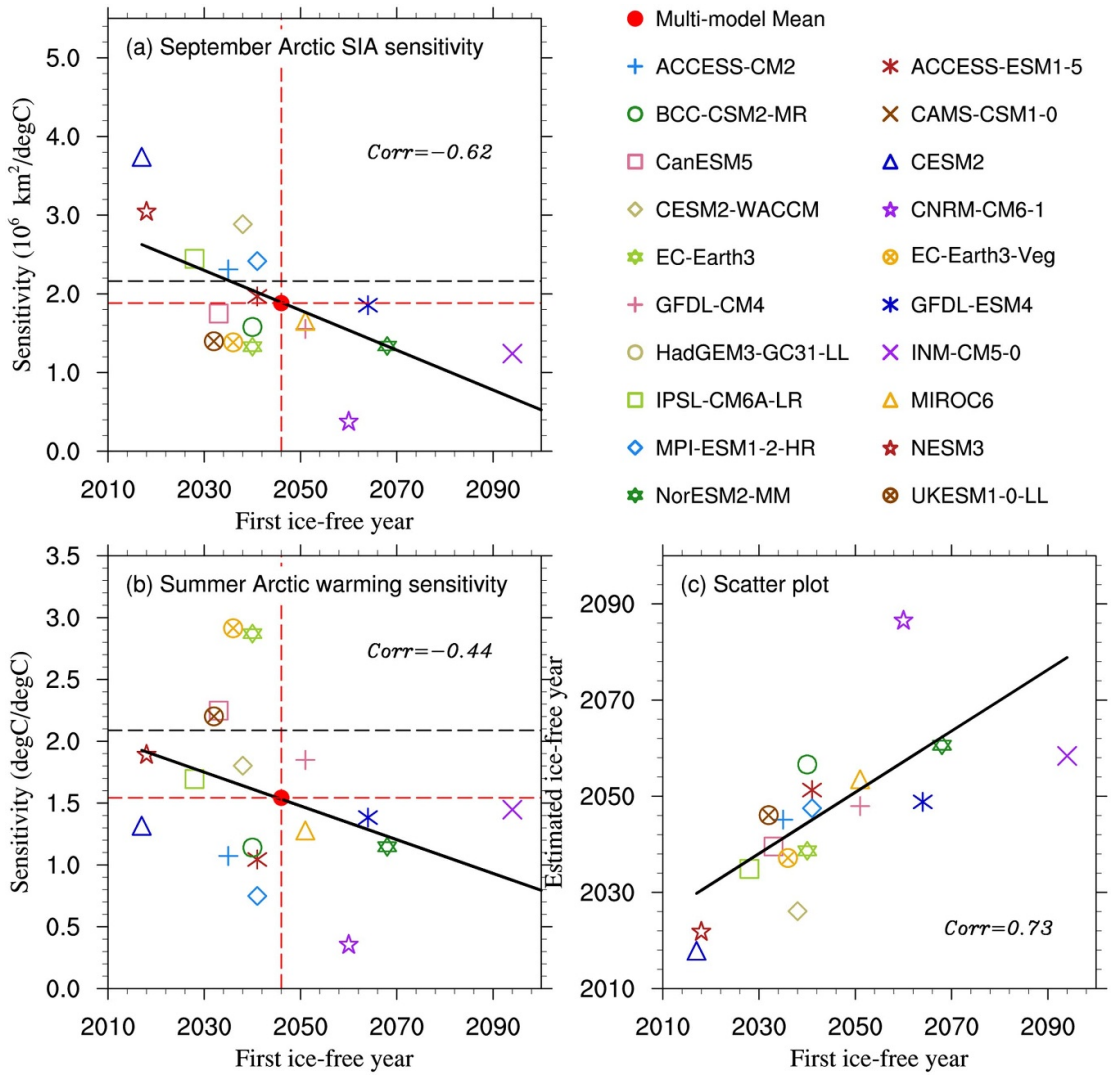

Figure 5. Relationship between the two sensitivity constraints and the projected first Arctic ice-free year under the SSP5-8.5 scenario: (a) September Arctic SIA sensitivity, and (b) Summer Arctic warming sensitivity. The black dashed line shows the observed sensitivity. The red dashed line denotes the multi-model ensemble mean. The models located above the red line means their sensitivities are comparable to the observed, so they are called realistic-sensitivity models. The models below the red line are called underestimated-sensitivity models. The linear regression lines and corresponding correlation coefficients are also shown in the panels (a) and (b). Panel (c) shows the scatter plot for the model projected ice-free year (abscissa) and the estimated ice-free year (ordinate) based on the two constraints.

4. Conclusion and discussion

The two complementary emergent constraints proposed here measure the models' capability in simulating realistic Arctic sea ice response to the local warming and the global atmospheric response to anthropogenic forcing in allocating heat to the Arctic region. The application of the two climate sensitivity constraints to CMIP6 models has resulted in a substantial reduction of projection uncertainties. The standard deviation of the ten realistic-sensitivity models' spread is reduced to about 30% of the ten underestimate-sensitivity models' counterparts. The ten realistic-sensitivity models' projections indicate that under the SSP2-4.5 scenario, eight out of ten models project that the Arctic ice-free year will occur before 2040 (figure 4(b)). The corresponding projected GMST in 2040 is 0.8 °C higher than in 2019. Similarly, under the SSP5-8.5 scenario, about 80% of realistic-sensitivity models project the first ice-free year before 2038 or about 0.8 °C above the 2019 level. The consistent projection result means that the first Arctic ice-free year's chance to occur with 0.8 °C further warmings is about 80%. This 0.8 °C additional warming based on the 2019 level equals about 1.9 °C from the pre-industrial level.

The sources of uncertainty primarily come from the model physics, internal variability, and the assumed emission scenarios. The scenario-independent climate sensitivity can reduce uncertainty originated from the emission pathway and allow better focusing on reducing the uncertainties

due to models' representing the physical and biogeochemical processes and the internal coupled variability. The influence of internal variability on individual observables cannot be reproduced by models, which poses an intrinsic difficulty in searching for emergent constraints solely based on observations. Notz (2015) pointed out that the usefulness of a climate-model simulation cannot be inferred solely from its degree of agreement with observations. This is particularly the case for the Arctic ice-free year that varies nonlinearly with time and contains considerable internal variability. Also, the observation involves significant uncertainty due to the quality and the limited number of years of the observations. Jahn *et al* (2016) have performed large ensemble experiments with the Community Earth System Model and shown that internal variability alone can lead to a prediction uncertainty of about two decades, while scenario uncertainty could add at least another five years. At this stage, all emergent constraints for estimating sea ice decline using observations involve uncertainties due to internal variability. There is an urgent need to seek ways to reduce the impact of internal variability on emergent constraints. Besides, large-ensemble runs are needed to reduce the internal variability-induced uncertainty (Murphy *et al* 2014, Sigmond and Fyfe 2016).

The inter-model spread analysis suggests that the projections' uncertainties may arise from the models' Arctic SIA sensitivity and Arctic warming sensitivities (figure 5). About half of CMIP6 models underestimate the Arctic SIA sensitivity and Arctic warming sensitivity (figure 4(a)). There is an urgent need to simulate accurate Arctic sea ice response to local surface temperature and the Arctic amplification ratio. Since the reduction of multi-model projection uncertainties is a common demand in projecting future changes, the proposed principle for establishing physics-based, complimentary emergent constraints through numerical experiments may provide the application to other climate fields to reduce projection uncertainty and understand uncertainty sources.

Data availability statement

All data that support the findings of this study are included within the article (and any supplementary files).

Acknowledgments

B Wang acknowledges the support by the National Science Foundation (Climate Dynamics Division) Award No. 2025057 and National Natural Science Foundation of China (Grant No. 91437218). Q Ding was supported by NSF's Polar Programs (OPP-1744598) and Modeling, Analysis, Predictions and Projections (NA19OAR4310281) and Ocean Observing and Monitoring (NA18OAR4310424) programs as part of NOAA's Climate Program Office. J Liu was supported by the Climate Program Office, NOAA, U.S. Department of Commerce (NA15OAR4310163). This paper is the IPRC publication #XXXX, SOEST publication #YYYYY, and ESMC publication #ZZZ.

Conflict of interest

The authors declare no conflict of interest.

Author contributions

B Wang initialized and wrote the manuscript, X Zhou conducted all data analysis and numerical experiments and helped write Q Ding and J Liu provided valuable comments and revisions of the manuscript.

References

Brient F 2020 Reducing uncertainties in climate projections with emergent constraints: concepts, examples and prospects *Adv. Atmos. Sci.* **37** 1–15

Cavalieri D J and Parkinson C L 2012 Arctic sea ice variability and trends, 1979–2010 *Cryosphere* **6** 881–9

Cohen J *et al* 2019 Divergent consensuses on Arctic amplification influence on midlatitude severe winter weather *Nat. Clim. Change* **10** 20–9

Comiso J C, Parkinson C L, Gersten R and Stock L 2008 Accelerated decline in the Arctic sea ice cover *Geophys. Res. Lett.* **35** L01703

Comiso J 2017 Bootstrap Sea Ice Concentrations from Nimbus-7 SMMR and DMSP SSM/I-SSMIS, Version 3 NASA National Snow and Ice Data Center Distributed Active Archive Center

Curry J A, Schramm J L and Ebert E E 1995 Sea Ice-Albedo climate feedback mechanism *J. Clim.* **8** 240–7

Ding Q *et al* 2017 Influence of high-latitude atmospheric circulation changes on summertime Arctic sea ice *Nat. Clim. Change* **7** 289–95

Döscher R, Vihma T and Maksimovich E 2014 Recent advances in understanding the Arctic climate system state and change from a sea ice perspective: a review *Atmos. Chem. Phys.* **14** 13571–600

Francis J A and Vavrus S J 2012 Evidence linking Arctic amplification to extreme weather in mid-latitudes *Geophys. Res. Lett.* **39** L06801

Gautier A 2020 Arctic sea ice decline stalls out at second lowest minimum *Arctic Sea Ice News and Analysis National Snow and Ice Data Center*

Graversen R G, Mauritsen T, Tjernström M, Källén E and Svensson G 2008 Vertical structure of recent Arctic warming *Nature* **451** 53–6

Gregory J M, Stouffer R J, Raper S C B, Stott P A and Rayner N A 2002 An observationally based estimate of the climate sensitivity *J. Clim.* **15** 3117–21

Grunseich G and Wang B 2016a Arctic sea ice patterns driven by the Asian summer monsoon *J. Clim.* **29** 9097–112

Grunseich G and Wang B 2016b Predictability of Arctic annual minimum sea ice patterns *J. Clim.* **29** 7065–88

He X and Hu M 2018 Review of the impact of the Arctic passage on the world trade pattern *Mar. Econ.* **7** 57–64

Herrington T and Zickfeld K 2014 Path independence of climate and carbon cycle response over a broad range of cumulative carbon emissions *Earth Syst. Dyn.* **5** 409–22

Hersbach H *et al* 2019 Global reanalysis: goodbye ERA-Interim, hello ERA5 (available at: www.ecmwf.int)

Hunke E, Lipscomb W, Jones P, Turner A, Jeffery N and Elliott S 2017 CICE, The Los Alamos sea ice model (available at: www.osti.gov)
Idso S B and Jackson R D 1969 Thermal radiation from the atmosphere *J. Geophys. Res.* **74** 5397–403
Jahn A 2018 Reduced probability of ice-free summers for 1.5 °C compared to 2 °C warming *Nat. Clim. Change* **8** 409–13
Jahn A, Kay J E , Holland M M and Hall D M 2016 How predictable is the timing of a summer ice-free Arctic? *Geophys. Res. Lett.* **43** 9113–120
Kanamitsu M, Ebisuzaki W, Woollen J, Yang S-K, Hnilo J J, Fiorino M and Potter G L 2002 NCEP–DOE AMIP-II reanalysis (R-2) *Bull. Am. Meteorol. Soc.* **83** 1631–44
Kay J E, Holland M M and Jahn A 2011 Inter-annual to multi-decadal Arctic sea ice extent trends in a warming world *Geophys. Res. Lett.* **38** L15708
Liu J, Song M, Horton R M and Hu Y 2013 Reducing spread in climate model projections of a September ice-free Arctic *Proc. Natl Acad. Sci.* **110** 12571–6
Mahlstein I and Knutti R 2012 September Arctic sea ice predicted to disappear near 2 °C global warming above present *J. Geophys. Res. Atmos.* **117** D06104
Massonnet F, Vancoppenolle M, Goosse H, Docquier D, Fichefet T and Blanchard-Wrigglesworth E 2018 Arctic sea-ice change tied to its mean state through thermodynamic processes *Nat. Clim. Change* **8** 599–603
Murphy J M, Booth B B B, Boulton C A, Clark R T, Harris G R, Lowe J A and Sexton D M H 2014 Transient climate changes in a perturbed parameter ensemble of emissions-driven earth system model simulations *Clim. Dyn.* **43** 2855–85
Notz D 2015 How well must climate models agree with observations? *Phil. Trans. R. Soc.* A **373** 20140164
Notz D (SIMIP Community) 2020 Arctic sea ice in CMIP6 *Geophys. Res. Lett.* **47** e2019GL086749
Notz D and Stroeve J 2016 Observed Arctic sea-ice loss directly follows anthropogenic CO_2 emission *Science* **354** 747–50
Olonscheck D, Mauritsen T and Notz D 2019 Arctic sea-ice variability is primarily driven by atmospheric temperature fluctuations *Nat. Geosci.* **12** 430–4
Overland J E, Wood K R and Wang M 2011 Warm Arctic—cold continents: climate impacts of the newly open *Arctic Sea Polar Res.* **30** 15787
Rosenblum E and Eisenman I 2016 Faster Arctic sea ice retreat in CMIP5 than in CMIP3 due to volcanoes *J. Clim.* **29** 9179–88
Serreze M C and Francis J A 2006 The Arctic amplification debate *Clim. Change* **76** 241–64
Shindell D and Faluvegi G 2009 Climate response to regional radiative forcing during the twentieth century *Nat. Geosci.* **2** 294–300
Sigmond M and Fyfe J C 2016 Tropical Pacific impacts on cooling North American winters *Nat. Clim. Change* **6** 970–4
Sigmond M, Fyfe J C and Swart N 2018 Ice-free Arctic projections under the Paris Agreement *Nat. Clim. Change* **8** 404–8
Smith L C and Stephenson S R 2013 New Trans-Arctic shipping routes navigable by midcentury *Proc. Natl Acad. Sci.* **110** E1191–5
Snape T J and Forster P M 2014 Decline of Arctic sea ice: evaluation and weighting of CMIP5 projections *J. Geophys. Res. Atmos.* **119** 546–54
Stroeve J C, Kattsov V, Barrett A, Serreze M, Pavlova T, Holland M and Meier W N 2012 Trends in Arctic sea ice extent from CMIP5, CMIP3 and observations *Geophys. Res. Lett.* **39** L16502
Stroeve J C, Serreze M C, Holland M M, Kay J E, Malanik J and Barrett A P 2011 The Arctic's rapidly shrinking sea ice cover: a research synthesis *Clim. Change* **110** 1005–27
Stroeve J and Notz D 2015 Insights on past and future sea-ice evolution from combining observations and models *Glob. Planet Change* **135** 119–32
Thackeray W and Hall A 2019 An emergent constraint on future Arctic sea-ice albedo feedback *Nat. Clim. Change* **9** 972–8
Wang M and Overland J E 2009 A sea ice free summer Arctic within 30 years? *Geophys. Res. Lett.* **36** L07502
Wang M and Overland J E 2012 A sea ice free summer Arctic within 30 years: an update from CMIP5 models *Geophys. Res. Lett.* **39** L18501